

Polynomial model inversion control: numerical tests and applications

C. Novara

Abstract—A novel control design approach for general nonlinear systems is described in this paper. The approach is based on the identification of a polynomial model of the system to control and on the on-line inversion of this model. Extensive simulations are carried out to test the numerical efficiency of the approach. Numerical examples of applicative interest are presented, concerned with control of the Duffing oscillator, control of a robot manipulator and insulin regulation in a type 1 diabetic patient.

I. INTRODUCTION

Consider a nonlinear discrete-time system in regression form:

$$y_t = h(u_t^-, y_t^-, \xi_t^-) \quad (1)$$

$$\begin{aligned} u_t^- &\doteq (u_{t-1}, \dots, u_{t-n}) \\ y_t^- &\doteq (y_{t-1}, \dots, y_{t-n}) \\ \xi_t^- &\doteq (\xi_{t-1}, \dots, \xi_{t-n}) \end{aligned}$$

where $u_t \in U \subset \mathbb{R}^{n_u}$ is the known input, $y_t \in \mathbb{R}^{n_y}$ is the measured output, $\xi_t \in \Xi \subset \mathbb{R}^{n_\xi}$ is an unmeasured disturbance; n is the system order; U and $\Xi \doteq \{\xi \in \mathbb{R}^{n_\xi} : \|\xi\| \leq \bar{\xi}\}$ are compact sets; the function h is Lipschitz continuous on $\Omega_h \doteq Y^n \times U^n \times \Xi^n$, where Y is a compact set. U accounts for possible constraints on u_t .

Suppose that the system (1) is unknown, but a set of noise-corrupted measurements is available:

$$\mathcal{D} \doteq \{\tilde{y}_t, \tilde{u}_t\}_{t=1-L}^0 \quad (2)$$

where the tilde is used to denote the samples of the data set \mathcal{D} .

Let $\mathcal{Y}^0 \subseteq Y^n$ be a set of initial conditions of interest, $\mathcal{R} \doteq \{\mathbf{r} = (r_1, r_2, \dots) : r_t \in Y, \forall t\}$ a set of output sequences of interest, and $\mathcal{E} \doteq \{\boldsymbol{\xi} = (\xi_1, \xi_2, \dots) : \xi_t \in \Xi, \forall t\}$ the set of all possible disturbance sequences.

The problem is to design a controller for the system (1) such that, for any $\boldsymbol{\xi} = (\xi_1, \xi_2, \dots) \in \mathcal{E}$, and for any initial condition $y_0 \in \mathcal{Y}^0$, the output sequence $\mathbf{y} = (y_1, y_2, \dots)$ of the controlled system tracks any reference sequence $\mathbf{r} = (r_1, r_2, \dots) \in \mathcal{R}$.

To solve this problem, a novel data-driven control approach will be described in the following, based on the identification of a polynomial prediction model and on the online inversion of this model via the efficient solution of suitable optimization problems. A simplified version of the approach is presented in [2].

II. DATA-BASED PREDICTION MODEL

A model is considered, of the form

$$y^+ = f(u^+, q^-) \quad (3)$$

where $y^+ \equiv y_t^+$ is a prediction of the system output (over some finite time horizon), $u^+ \equiv u_t^+$ is a vector with the present and future input values and $q^- \equiv q_t^- \doteq (u_t^-, y_t^-)$. The subscript indicating the time will be omitted in the remainder of the paper when not necessary. A parametric structure is taken for the vector-valued function f . In particular, each component f_j of f is parametrized as

$$f_j(\cdot) = \sum_{i=1}^N \alpha_{ij} \phi_i(\cdot) \quad (4)$$

where ϕ_i are polynomial basis functions, α_{ij} are parameters to be identified and $j = 1, \dots, \tau n_y$. The parameters α_{ij} can be identified from the data (2) by means of convex optimization.

III. POLYNOMIAL INVERSION CONTROL

The proposed control approach is based on the on-line inversion of the model (3): at each time $t > 0$, given a reference sequence r^+ and the current regressor q^- , a command sequence u^+ is looked for, such that the model output \hat{y}^+ is “close” to r^+ :

$$\hat{y}^+ = f(u^+, q^-) \cong r^+. \quad (5)$$

Such a command sequence is found solving the optimization problem

$$u^* = \arg \min_{u \in U^\tau} J(u, r^+, q^-) \quad (6)$$

where

$$J(u, r^+, q^-) \doteq \|r^+ - f(u, q^-)\|_2^2 + \mu \|u\|_2^2 \quad (7)$$

and $\mu \geq 0$ is a design parameter, determining the trade-off between tracking precision and command activity.

The problem (6) is solved at each sampling time, resulting in the following control law:

$$u_t^* = u_{end}^* \equiv u_{end}^*(r_t^+, q_t^-) \quad (8)$$

where u_{end}^* is the first entry of the vector u^* in (6).

The objective function (7) is in general non-convex. Moreover, the optimization problem (6) has to be solved on-line, and this may require a long time compared to the sampling time used in the application of interest. To overcome these relevant problems, three algorithms have been developed, allowing an efficient computation of the optimal command input u_t^* for the following cases:

- 1) SIMO system and piecewise constant command input; the optimal solution can be computed “almost analytically”.
- 2) MIMO system affine in u^+ ; the cost function is convex, implying that the optimal solution can be obtained with “low” computational cost.
- 3) General MIMO system. we will show below by means of extensive simulations that the algorithm is able to find always a solution “very close” to a global one, in very short times.

The algorithms are based on a coordinate minimization approach but are not described here.

IV. OPTIMIZATION ALGORITHM PERFORMANCE EVALUATION

The optimization problem 6 was considered, where $f(\cdot)$ is a polynomial function of degree d_p and $u \in U \subset \mathbb{R}^m$, $r^+, q^- \in \mathbb{R}^m$. This problem is analogous to (6) but the dependence on time is not evidenced. The value $\mu = 0$ was taken since, with this value, if r^+ is in the range of $f(\cdot)$, we know the global minimum of $J(u, r^+, q^-)$ to be 0.

Values of m in the set $\{1, 2, 4, 6, 8\}$ and values of d_p in the set $\{1, 2, 4, 6\}$ were considered, corresponding to MIMO systems with up to 8 command inputs and models with polynomial degree up to 6. Note that in all the applications presented below, degrees $2 \div 4$ led to a very satisfactory prediction and control performance. Degrees larger than 4 seem in general to not give any advantage.

For each combination of m and d_p in these sets, a Monte Carlo simulation was carried out, consisting of 50 main trials, each consisting of 100 sub trials (total number of trials: $5 * 4 * 50 * 100 = 100\,000$).

In each main trial, $f(\cdot)$ was defined as a polynomial function of degree d_p with sparse random coefficients. In particular, a number n_s of nonzero coefficients was assumed, with n_s ranging in the interval $[0, 500]$ in function of m and d_p (the nonzero coefficients were chosen according to a Gaussian distribution with zero mean and unitary variance). In each sub trial, a sequence $r_i = f(u_i^{true}, q_i^-)$ was generated, where q_i^- and u_i^{true} are vectors with random entries (chosen according to a uniform distribution with support $[-1, 1]$), and $i = 1, \dots, 100$. Then, for each i , the optimization problem (6) was solved. Note that the decision variable u is different from the “true” input u_i^{true} .

For each combination of the dimension m and the polynomial degree d_p , the following indexes were considered to evaluate the algorithm performance:

- $E_2 \doteq \frac{1}{5000} \sum_{i=1}^{5000} (J(u_i^*, r_i^+, q_i^-) - J(u_i^{true}, r_i^+, q_i^-))$, where u_i^* is the solution of the optimization problem (6), computed for each random sample. Note that, in the present case, we know that $J(u_i^{true}, r_i^+, q_i^-) = 0$.
- $E_\infty \doteq \max_{i=1, \dots, 5000} (J(u_i^*, r_i^+, q_i^-) - J(u_i^{true}, r_i^+, q_i^-))$.
- $T_{sc} \doteq$ average time taken by a Matlab .m function to solve a single optimization problem on a laptop with an i7 3Ghz processor and 16 MB RAM. The average was computed over the 5000 samples of the Monte Carlo simulation.

- $T_m \doteq$ average time taken by a compiled Simulink mex function to solve a single optimization problem on the same laptop. This function was generated in 10 of the 50 main trials, since this operation is relatively complex. The average was thus computed over $10 * 100 = 1000$ samples of the Monte Carlo simulation.

The obtained results are summarized in Table I. It can be concluded that the coordinate descent minimization approach is able to find precise solutions (i.e., giving small values of the objective function) in short times for all the considered input dimensions and polynomial degrees. It can also be observed that using compiled mex functions allows a significant reduction of the computation times for problems involving polynomials with a not too high degree in u . A possible interpretation is that the Simulink automatic compiler loses efficiency for large degree polynomials.

m	d_p	n_s	E_2	E_∞	T_{sc} [s]	T_m [s]
1	1	3	1.2e-14	3.2e-14	2.7e-4	<1.0e-4
	2	6	1.9e-13	1.9e-12	3.0e-4	<1.0e-4
	4	15	2.1e-13	1.4e-12	3.4e-4	<1.0e-4
	6	28	1.1e-13	6.5e-13	3.7e-4	<1.0e-4
2	1	5	4.3e-12	1.6e-11	8.7e-4	<1.0e-4
	2	15	5.0e-3	0.048	1.6e-3	1.4e-4
	4	45	4.1e-3	0.022	2.2e-3	5.6e-4
	6	81	5.2e-3	0.034	5.4e-3	> T_{sc}
4	1	9	7.5e-5	4.2e-4	7.8e-4	<1.0e-4
	2	45	8.2e-3	0.039	3.1e-3	4.5e-4
	4	116	0.013	0.047	0.038	> T_{sc}
	6	197	0.014	0.046	0.17	> T_{sc}
6	1	13	4.3e-4	9.7e-4	1.9e-3	<1.0e-4
	2	81	0.013	0.048	0.011	1.2e-3
	4	197	0.016	0.048	0.21	> T_{sc}
	6	339	0.021	0.049	0.76	> T_{sc}
8	1	17	5.0e-4	8.6e-4	2.4e-3	<1.0e-4
	2	116	0.019	0.048	0.10	3.1e-3
	4	289	0.027	0.049	1.6	> T_{sc}
	6	500	0.032	0.049	8.3	> T_{sc}

Table I
MONTE CARLO SIMULATION RESULTS.

V. APPLICATIONS

A. Duffing oscillator

The Duffing system is a second-order damped oscillator with nonlinear spring, described by the following differential equations:

$$\begin{aligned} \dot{x}_1 &= x_2 \\ \dot{x}_2 &= -\alpha_1 x_1 - \alpha_2 x_1^3 - \beta x_2 + u \\ y &= x_1 + \xi \end{aligned} \quad (9)$$

where $x = (x_1, x_2)$ is the system state (x_1 and x_2 are the oscillator position and velocity, respectively), u is the input, y is the output, and ξ is a zero-mean Gaussian noise having a noise-to-signal standard deviation ratio of 0.03. The following values of the parameters have been considered: $\alpha_1 = -1$, $\alpha_2 = 1$, $\beta = 0.2$. For these parameter values and for certain choices of the input signal, this system exhibits a chaotic behavior, and this makes control design a particularly challenging problem.

A simulation of the Duffing system (9) having duration 400 s was performed, using the input signal $u(\tau) = 0.3 \sin(\tau) +$

$\xi^u(\tau)$, where τ here denotes the continuous time and $\xi^u(\tau)$ is a white Gaussian noise with zero mean and standard deviation 0.2.

A set of $L = 4000$ data were collected from this simulation with a sampling period $T_s = 0.1$ s:

$$\mathcal{D} \doteq \{\tilde{u}_t, \tilde{y}_t\}_{t=-1999}^0$$

where $\tilde{u}_t = u(T_s t)$ are the measurements of the input and $\tilde{y}_t = y(T_s t)$ are the measurements of the output.

A nonlinear controller was designed following the approach described in Sections II and III. This controller was applied to the Duffing system (9).

A testing simulation of the controlled system with duration 800 s was performed, using zero initial conditions and a reference signal r_t generated as a sequence of random steps, filtered by a second-order filter with a cutoff frequency of 2 rad/s (this filter has been inserted in order to ensure not too abrupt variations). A Gaussian noise affecting the output measurements, having zero-mean and a noise-to-signal standard deviation ratio of 0.03 was included in the simulation. In Figure 1, the output of the controlled system is compared to the reference.

Then, a Monte Carlo simulation was carried out, where this data-generation-control-design-and-testing procedure was repeated 100 times. For each trial, the tracking performance was evaluated by means of the Root Mean Square tracking error

$$RMS \doteq \sqrt{\frac{1}{8000} \sum_{t=1}^{8000} (r_t - y_t)^2}.$$

The average RMS error obtained in the Monte Carlo simulation is $\overline{RMS} = 0.015$.

A simulation of the closed-loop system was also performed where $r_t = 0, \forall t$ and ξ_t was a step disturbance of amplitude 0.5. The output signals obtained in these simulations are shown in Figure 2.

From these results, it can be concluded that the designed controller is able to (1) ensure a very accurate tracking, even in the presence of quite significant measurement noises; (2) reject/attenuate strong step disturbances.

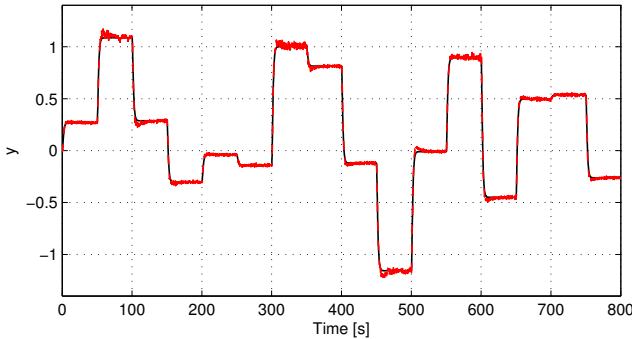


Figure 1. Tracking performance of the controlled system. Continuous (black) line: reference. Dashed (red) line: actual output.

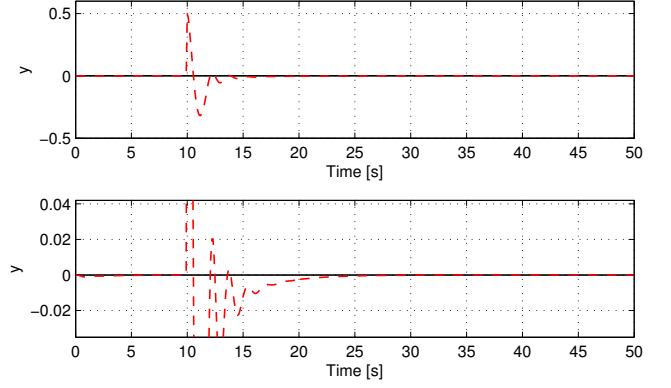


Figure 2. Above: disturbance rejection of the controlled system. Below: same figure, with zoomed y axis. Continuous (black) line: reference. Dashed (red) line: actual output.

B. Robot manipulator

The 2-DOF (2-degrees of freedom) robot manipulator depicted in Figure 3 has been considered, where ζ_1 and ζ_2 are the angular positions of the two segments of the robot arm, u_1 and u_2 are the control torques acting on these segments, l_1 and l_2 are the segment lengths, and M_1 and M_2 are the segment masses. The parameter values $l_1 = 0.8$ m, $l_2 = 0.7$ m, $M_1 = 2.5$ Kg, $M_2 = 2$ Kg have been assumed.

This robot manipulator is a MIMO system (with 2 inputs and 2 outputs), described by the following continuous-time state-space nonlinear equations:

$$\begin{aligned} \dot{z}(\tau) &= A^c(z(\tau))z(\tau) + B^c(z(\tau))u(\tau) \\ y(\tau) &= \begin{bmatrix} z_1(\tau) \\ z_2(\tau) \end{bmatrix} \end{aligned} \quad (10)$$

where τ is the continuous time, $z(\tau) = [\zeta_1(\tau) \zeta_2(\tau) \dot{\zeta}_1(\tau) \dot{\zeta}_2(\tau)]^T$ is the state, $u(\tau) = [u_1(\tau) u_2(\tau)]^T$ is the input, and the expressions of $A^c(z(\tau)) \in \mathbb{R}^{4 \times 4}$ and $B^c(z(\tau)) \in \mathbb{R}^{4 \times 2}$ can be found in [3].

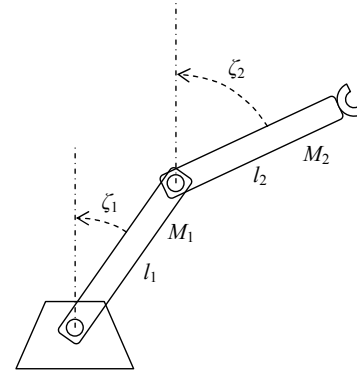


Figure 3. Robot Manipulator.

A set of $L = 5000$ data was generated by simulation of (10):

$$\mathcal{D} \doteq \{\tilde{y}_t, \tilde{u}_t\}_{k=-4999}^0.$$

The data were collected with a sampling time $T_s = 0.02$ s,

using the following input signals:

$$u_j(\tau) = \begin{cases} -20z_j(\tau), & \text{if } |z_j(\tau)| \geq 1.75 \text{ rad} \\ 0, & \text{if } l < \tau \leq l + 500, l = 500, 1500, 2500, 3500, \\ & \text{and } |z_j(\tau)| < 1.75 \\ U \sin(\omega_{j1}\tau) + U \sin(\omega_{j2}\tau), & \text{otherwise,} \end{cases} \quad (11)$$

where $j = 1, 2$, $U = \text{rand}[50, 150]$ Nm, $\omega_{11} = \text{rand}[0.05, 0.09]$ rad/s, $\omega_{12} = \text{rand}[0.5, 0.11]$ rad/s, $\omega_{21} = \text{rand}[0.04, 0.1]$ rad/s, $\omega_{22} = \text{rand}[0.7, 1.2]$ rad/s. The notation $U = \text{rand}[50, 150]$ means that U is a number, randomly chosen according to a uniform distribution in the interval $[50, 150]$. The feedback input on the first line of (11) was applied in order to limit the working range of z_1 and z_2 to the interval $[-\pi, \pi]$ rad (the gain -20 and the threshold 1.75 rad were chosen through several preliminary simulations). Measurement noises were added to y_j , $j = 1, 2$, simulated as uniform noises with amplitude 0.02 rad.

From these data, two controllers were designed following the approach described in Sections II and III: The first one is based on a general nonlinear prediction model. The second one is based on a prediction model affine in u^+ . For comparison, the controller in [4] has been considered, designed by means of a two-step method, consisting in LPV model identification and Gain Scheduling (GS) design.

A first simulation was performed to test all the controllers in the task of reference tracking. Zero initial conditions were assumed. A reference signal of length 5000 samples (corresponding to 100 s) was used, defined as a random sequence of step signals with amplitudes in the interval $[-\pi, \pi]$, filtered by a second-order filter with a cutoff frequency of 10 rad/s. This filter was inserted in order to ensure not too high variations. The outputs were corrupted by random uniform noises with amplitude 0.02 rad. In Figure 4, the angular positions of the closed-loop system with the first controller are compared with the references for the first 20 s of this simulation. Note that the two position references were chosen quite similar to each other (but not equal) in order to allow the manipulator to reach in a simple way any position in its range. A second simulation was performed to test the controllers in the task of disturbance attenuation. Zero initial conditions and a zero reference were assumed. An output disturbance signal of length 1000 samples (corresponding to 20 s) was considered, defined as a sequence of two steps (one for each output channel) of amplitude 1 rad, filtered by a second-order filter with a cutoff frequency of 10 rad/s. The outputs were also corrupted by random uniform noises with amplitude 0.02 rad. In Figure 5, the angular positions of the closed-loop system with the first controller are shown, together with the disturbance signals.

Then, a Monte Carlo (MC) simulation was carried out, where this procedure (data generation, control design, reference tracking test) was repeated 200 times. For each trial, the tracking performance was evaluated by means of the Root Mean Square tracking errors, defined as

$$RMS_i \doteq \sqrt{\frac{1}{5000} \sum_{t=1}^{5000} (r_{i,t} - y_{i,t})^2}, \quad i = 1, 2,$$

where $r_{i,t}$ is the i th component of the reference signal and $y_{i,t}$ is the i th component of the controlled system output. The average errors \overline{RMS}_i obtained in the MC simulation are reported in Table II. From these results, it can be concluded that the designed control systems are quite effective, showing a fast and precise tracking, and a significant disturbance attenuation capability. In comparison with the two-step method of [4], the proposed approach is simpler, since a polynomial model of the form (3) has in general a significantly simpler structure wrt an LPV model (and, in particular, wrt a state-space LPV model). Moreover, the tracking results obtained by the inversion-based controllers are similar (or even slightly better) than those obtained by the GS controller, despite the fact that this latter uses a stronger information on the system (10) (i.e., the information that (10) is a quasi-LPV system). The computational times for the control design phase (referred to a laptop with an i7 3GHz processor and 16 MB RAM) resulted quite low, considering that the set used for design consists of 5000 data: 92 s (nonlinear model), 83 s (affine model). The control algorithm on-line evaluation times resulted also quite low: $2.1 \cdot 10^{-3}$ s (nonlinear model), $1.0 \cdot 10^{-3}$ s (affine model). This shows that these algorithms can be effectively implemented on real time processors.

	controller 1	controller 2	GS
RMS_1	0.159	0.160	0.167
RMS_2	0.114	0.115	0.152

Table II
ROBOT MANIPULATOR. AVERAGE RMS TRACKING ERRORS.

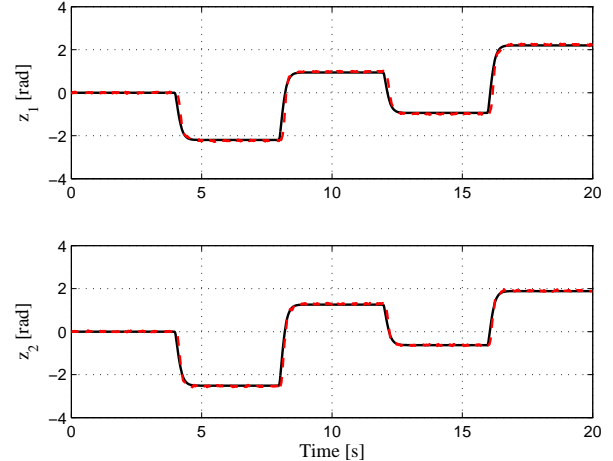


Figure 4. Robot Manipulator. Continuous (black) line: reference. Dashed (red) line: closed-loop system output.

C. Type 1 diabetes

A model representing a type 1 diabetic patient has been considered in this example. The inputs of this model are the carbohydrate-based meal input and the insulin input function, the output is the blood glucose concentration (glycemic response). The model state equations are the following:

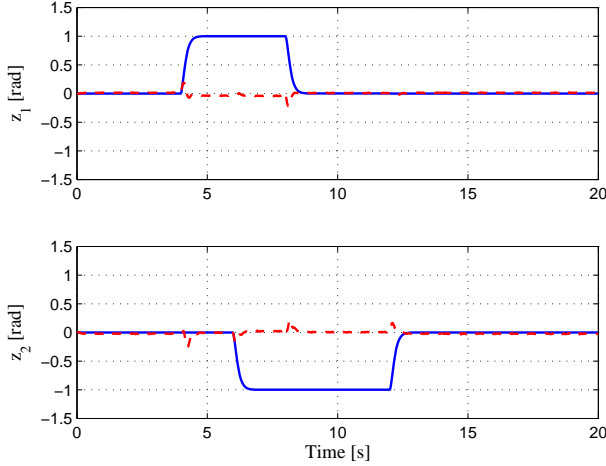


Figure 5. Robot Manipulator. Continuous (blue) line: disturbance. Dashed (red) line: closed-loop system output.

$$\begin{aligned}
 \frac{dy(t)}{dt} &= -[p_1 + \eta(t)]y(t) + p_1 G_b + \frac{1}{V_g}w(t) \\
 \frac{d\eta(t)}{dt} &= -p_2\eta(t) + p_3[I(t) - I_b] \\
 \frac{dI(t)}{dt} &= \frac{k_a}{V_d}I_2(t) - k_e I(t) \\
 \frac{dI_1(t)}{dt} &= -k_{21}I_1(t) + \frac{1}{V_I}u(t) \\
 \frac{dI_2(t)}{dt} &= k_{21}I_1(t) - (k_d + k_a)I_2(t)
 \end{aligned} \quad (12)$$

where $y(t)$ is the blood glucose concentration (the system output), $I(t)$ is the blood insulin concentration, $\eta(t)$ is the insulin concentration in a remote compartment, V_g is the volume distribution, $w(t)$ is the carbohydrate-based meal input (the system unmeasured input), $I_1(t)$ is the subcutaneous insulin mass in the injection depot, $I_2(t)$ is the subcutaneous insulin mass proximal to plasma and $u(t)$ is the injected insulin rate (the system measured input); p_1 , p_2 , p_3 are individual subject parameters, V_d is the plasma distribution volume, k_{21} , k_a , k_d , and k_e are insulin pharmacokinetic parameters, I_b is the basal blood insulin concentration and G_b is the basal blood glucose concentration.

The first two equations of (12), describing the glucose dynamics, have been taken from the Bergman model, [1]; the last three equations of (12), describing the insulin kinetics, have been taken from the Shimoda model, [5]. The following parameter values have been assumed: $p_1 = 0.031 \text{ min}^{-1}$, $p_2 = 0.012 \text{ min}^{-1}$, $p_3 = 9.56e - 6 \text{ min}^{-2} \text{ mL}/\mu\text{U}$, $V_g = 1.45 \text{ dL}/\text{kg}$, $V_d = 0.2 \text{ mL}/\text{kg}$, $V_I = 5e - 3 \text{ mL}$, $k_{21} = 0.0166 \text{ min}^{-1}$, $k_a = 0.0133 \text{ min}^{-1}$, $k_d = 0.0033 \text{ min}^{-1}$, $k_e = 0.3 \text{ min}^{-1}$, $I_b = 0 \mu\text{U}/\text{mL}$ and $G_b = 180 \text{ mg}/\text{dL}$. In this simulated example, the model (12) represents the unknown “true” patient metabolic system to control.

It must be remarked that the model (12) is not the most recent that can be found in the literature and may also be not sufficiently adequate to describe a real diabetes patient. However, the aim of this numerical example is to test the proposed control algorithm on a non trivial nonlinear system and thus the particular choice of the model used as the “true” system is not relevant.

A simulation of the patient system (12) was performed, where the insulin input was taken from a set of experimental data, measured on a real patient. The meal input was simulated as a superposition (with positive coefficients) of exponentially decaying signals $w_j(t)$ $j = 1, 2, \dots$, where each contribution $w_j(t)$ represents a single meal. These signals are of the form

$$w_j(t) = \begin{cases} 0, & t < t_j \\ (t - t_j) e^{-0.6(t-t_j)}, & t \geq t_j \end{cases} \quad (13)$$

where t_j is the time at which the patient started to eat. The times t_j were realistically chosen in order to have an insulin injection a few minutes before a meal. A negative term of the form (13) were also added to the meal input in order to reproduce the effects of an external input yielding a decrease of the output (e.g. a physical activity). The output signal (the blood glucose concentration) resulting from this simulation was corrupted by a white noise, having a noise-to-signal standard deviation ratio of 3%.

A set of $L = 4800$ data (corresponding to 10 days) was collected from this simulation, using a sampling time $T_s = 3 \text{ min}$:

$$\mathcal{D} \doteq \{\tilde{u}_t, \tilde{y}_t\}_{t=-4799}^0$$

where $\tilde{u}_t = u(T_s t)$ are the measurements of the insulin input and $\tilde{y}_t = y(T_s t)$ are the measurements of the output. Note that, as it happens in most real situations, the meal input was not measured.

A nonlinear controller was designed following the approach described in Sections II and III. This controller was applied to the diabetes system (12).

Three simulations of the patient system (12) with duration 10 days were performed, using a meal input signal different from that used to generate the design data \mathcal{D} . The insulin signal was generated as follows:

- first simulation: zero insulin;
- second simulation: insulin injected by the patient on the basis of his/hers experience;
- third simulation: insulin signal computed by the designed controller.

In the simulations, the output signal was corrupted by a white noise, with a noise-to-signal standard deviation ratio of 3%. The obtained results can be commented as follows: With no insulin, the glucose concentration becomes very large, leading to serious health problems of the patient. When the amount of injected insulin is decided by the patient, the glucose concentration is somewhat regulated but it may reach large values, which may worsen the patient health conditions (see Figure 6). When the amount of injected insulin is decided by the controller, the glucose concentration is always kept within the interval $[80, 180] \text{ mg}/\text{dL}$ which, in diabetes treatment medicine, is commonly considered a safe interval (see Figure 6).

REFERENCES

- [1] R N Bergman, L S Phillips, and C Cobelli. Physiologic evaluation of factors controlling glucose tolerance in man: measurement of insulin sensitivity and beta-cell glucose sensitivity from the response to intravenous glucose. *The Journal of Clinical Investigation*, 68(6):1456–1467, 12 1981.

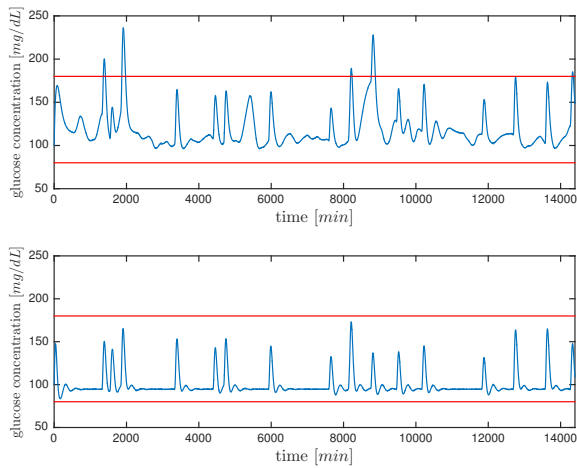


Figure 6. Blue lines: patient glucose concentration; red lines: safety bounds. Above: result with insulin signal decided by the patient; below: result with insulin signal generated by the controller.

- [2] S. Formentin, C. Novara, S.M. Savaresi, and M. Milanese. Active braking control system design: the d2-ibc approach. *IEEE/ASME Transactions on Mechatronics*, 20(4):1573–1584, 2015.
- [3] A. Kwiatkowski and H. Werner. LPV control of a 2-DOF robot using parameter reduction. In *Proceedings of the IEEE Conference on Decision and Control and European Control Conference*, Seville, Spain, 2005.
- [4] C. Novara. Set membership identification of state-space LPV systems. In P. Lopes dos Santos, T.P. Azevedo Perdicoulis, C. Novara, J.A. Ramos, and D.E. Rivera, editors, *Linear Parameter-Varying System Identification – New Developments and Trends, Advanced Series in Electrical and Computer Engineering Vol. 14*, pages 65–93. World Scientific, 2011.
- [5] Gianluca Nucci and Claudio Cobelli. Models of subcutaneous insulin kinetics. a critical review. *Computer Methods and Programs in Biomedicine*, 62(3):249 – 257, 2000.